Downregulation of triggering receptor expressed on myeloid cells 1 inhibits invasion and migration of liver cancer cells by mediating macrophage polarization

MINMIN CHEN*, RUIMIN LAI*, XIAOYU LIN, WEI CHEN, HUIZHEN WU and QI ZHENG

Department of Hepatology, Hepatology Research Institute, The First Affiliated Hospital, Fujian Medical University, Fuzhou, Fujian 350005, P.R. China

Received August 3, 2020; Accepted January 21, 2021

DOI: 10.3892/or.2021.7988

Abstract. Triggering receptor expressed on myeloid cells-1 (TREM1) is a cell-surface protein expressed on tumor-associated macrophages (TAMs), the predominant inflammatory cells in the tumor microenvironment; however, the mechanisms for the influence of TREM1 on TAM polarization during liver cancer progression have not been investigated. In the present study, 20 patients diagnosed with hepatocellular carcinoma (HCC) who underwent surgery were enrolled, and TREM1 expression on M1/M2 macrophages and on M2 macrophages was assessed by immunohistochemical staining. Human leukemia monocytic cells (THP-1) were differentiated into M2 macrophages using phorbol 12-myristate 13-acetate, IL-4 and IL-13. A specific short hairpin RNA was used to knockdown TREM1 expression. To investigate the effects of TREM1 downregulation in macrophages on the migration and invasion of liver cancer cells, HepG2 and MHCC97H cell lines were co-cultured with specific conditioned media. Reverse transcription-quantitative PCR and western blot analyses were used to detect M1 and M2 macrophage marker expression. The expression levels of proteins of the PI3K/AKT/mTOR signaling pathway were analyzed by western blotting, revealing that TREM1 expression in HCC tissues was significantly elevated compared with that in adjacent normal tissues, and TREM1 was highly expressed on the cell membranes of M2 macrophages in tumor tissues compared with in adjacent normal tissues. The present results demonstrated that TREM1 downregulation in macrophages shifted M2 macrophages towards an M1 phenotype, as defined by higher expression levels of M1-associated markers and decreased expression levels of M2-associated markers. In addition, TREM1 downregulation in macrophages suppressed migration and invasion of HepG2 and MHCC97H cells. Furthermore, TREM1-knockdown in macrophages inhibited PI3K/AKT/mTOR activation in the polarization of M2 macrophages. In conclusion, downregulation of TREM1 expression in macrophages shifted M2 macrophages towards a M1 phenotype via inhibiting PI3K/AKT signaling. In addition, migration and invasion of HepG2 and MHCC97H cells were inhibited when this signaling pathway was blocked. The present findings suggest TREM1 as a novel potential therapeutic target for liver cancer management.

Correspondence to: Dr Qi Zheng, Department of Hepatology, Hepatology Research Institute, The First Affiliated Hospital, Fujian Medical University, 20 Chazhong Road, Taijiang, Fuzhou, Fujian 350005, P.R. China
E-mail: zhengqi0825@sina.com

*Contributed equally

Abbreviations: Arg-1, arginase-1; CM, conditioned media; EMT, epithelial-mesenchymal transition; HCC, hepatocellular carcinoma; iNOS, inducible nitric oxide synthase; PMA, phorbol 12-myristate 13-acetate; shRNA, short hairpin RNA; TAMs, tumor-associated macrophages; TME, Tumor microenvironment; TREM1, triggering receptor expressed on myeloid cells-1

Key words: TREM1, TAMs, HCC, PI3K/AKT, macrophage

Introduction

Hepatocellular carcinoma (HCC) is one of the most notorious solid tumors and has become a rapidly increasing cause of cancer-associated death in the USA (1-3). Based on the 2018 Global Cancer Statistics, liver cancer has an incidence of 4.7% and a mortality rate of 8.2% (4). Although surgery, local ablation, trans-arterial chemoembolization and systemic therapy have greatly advanced treatment of patients with HCC (5), distant and intrahepatic metastasis and postoperative recurrence remain a concern and result in poor outcomes in these patients (6,7). Therefore, identifying or discovering novel early diagnostic biomarkers and elucidating the underlying mechanisms of cancer metastasis has received much focus for improving treatment efficacy and prognosis in patients with liver cancer.

HCC is an inflammation-associated cancer (8,9), with chronic inflammation closely associated with disease progression. Tumor-associated macrophages (TAMs) are predominantly inflammatory cells in the tumor microenvironment (TME) that serve a pivotal role in tumor initiation, metastasis, angiogenesis and suppression of adaptive immunity (10). In the TME, TAMs exhibit high plasticity and heterogeneity in response to different stimuli, existing as

classically activated macrophages (M1 macrophages) and alternatively activated macrophages (M2 macrophages) (11). In response to inflammatory mediators, M1 macrophages express inducible nitric oxide synthase (iNOS), which uses L-arginine as a substrate to produce nitric oxide (12), and exhibit pro-inflammatory and anti-tumorigenic properties. Conversely, M2 macrophages constitutively express the enzyme arginase-1 (Arg-1), which hydrolyzes L-arginine to L-ornithine (12) and demonstrates anti-inflammatory and pro-tumor characteristics. TAMs predominantly exhibit M2 properties with a pro-tumor phenotype (13), promote tumor cell proliferation, invasion, metastasis, neovascularization and suppression of the adaptive immune response in the TME (14,15). Therefore, identifying mechanisms through which macrophages are polarized in the TME is crucial for understanding their roles in tumor progression.

Triggering receptor expressed on myeloid cells (TREM) proteins are a family of immunoglobulin cell surface receptors expressed on myeloid cells that consist of a single extracellular immunoglobulin-like domain, a trans-membrane region and a short cytoplasmic tail (16). The TREM gene cluster is located on human chromosome 6p21, and includes genes that encode TREM1 and TREM2; on mouse chromosome 17c3, it encodes for TREM3 (16). TREM1 activation is associated with downstream signaling adaptor DNAX activation protein of 12 kDa (17) and peptidoglycan recognition protein-1 (18). TREM1 acts as a potent amplifier of inflammatory responses and leads to the increased secretion of pro-inflammatory cytokines, including monocyte chemotactic protein-1, TNFα, IL-1α, IL-1β, IL-6, IL-8 and macrophage colony-stimulating factor (19). In human non-small cell lung cancer, high expression levels of TREM1 on TAMs are associated with tumor recurrence and poor prognosis (20), suggesting that TREM1 may play an important role in cancer progression. In experimental xenograft mouse models of pancreatic cancer, inhibiting TREM1 attenuates tumor growth and prolongs survival (21). Similarly, in a chemically induced model of HCC, TREM1 serves a role in the connection between the activation of Kupffer cells and tumorigenesis (22). However, the role of TREM1 in the regulation of macrophage polarization in tumor-associated inflammation and its microenvironment has not been established. The present study aimed to investigate the influence and possible signaling pathway of TREM1 on macrophage polarization. Additionally, the effects of TREM1 downregulation in macrophages on the migration and invasion of liver cancer cells were explored.

Materials and methods

Patients and specimens. Incisional biopsy samples (tumor and adjacent normal tissues) were collected from 20 clinically diagnosed patients with HCC between August 2014 and April 2016, and were sent for histological confirmation according to classical histopathological features. The distance of the adjacent tissue from the tumor was >5 cm. Patients with other systemic tumors, infections or incomplete clinical data were excluded. All samples were obtained from the Department of Hepatobiliary Surgery of The First Affiliated Hospital of Fujian Medical University (Fuzhou, China). The mean age of the patients was 53 years (age range, 41-65 years). Clinical and laboratory parameters of patients such as disease severity were evaluated using the Child-Pugh score (23). Tumor staging was based on the Barcelona-Clinic Liver Cancer system (24). All patients signed informed consent forms in accordance with the Declaration of Helsinki. The study protocol was approved by the Ethical Committee of The First Affiliated Hospital of Fujian Medical University [approval no. (2015) 132].

Immunohistochemistry. For immunohistochemistry, three areas of tumor specimens and adjacent normal tissues from 20 patients with HCC were fixed with 10% formalin for 24 h at 37˚C and embedded in a paraffin block. Subsequently, the samples were de-paraffinized in two changes of xylene for 5 min each at 37˚C and rehydrated in 100, 95, 70 and 50% alcohol for 5 min each at 37˚C, and finally sectioned into 5-μm-thick slices. For antigen retrieval, samples were treated with 10 mM citrate buffer (pH 6.0) at 100˚C for 10 min. After quenching endogenous peroxidase with 3% hydrogen peroxide for 30 min at 37˚C, 0.5% bovine serum albumin (BSA; cat. no. ST025-5 g; Beyotime Institute of Biotechnology) was used for 1 h at 37˚C to block non-specific binding. The sections were then incubated overnight at 4˚C with polyclonal rabbit anti-human TREM1 antibody (1:200; cat. no. YT5133; ImmunoWay Biotechnology Company). Subsequently, the sections were incubated with the appropriate goat anti-rabbit IgG secondary antibody (1:1,000; cat. no. ab6721; Abcam) for 60 min at 37˚C according to the manufacturer's instructions. Images of the labeled specimens were captured with an Olympus CX41 light microscope (Olympus Corporation; magnification, x400) and analyzed using ImageJ software (v1.4; National Institutes of Health). All experiments were performed in triplicate.

Immunohistochemical double staining. Immunohistochemical double staining (CD206+Arg-1, CD16+iNOS and CD206+TREM1) was performed using the DouMaxVision• immunohistochemical double staining test kit (cat. no. KIT-9998; Fuzhou Maixin Biotech Co., Ltd.) according to the manufacturer's protocol, and the number of positively stained cells in five high-power fields was counted under an Olympus CX41 light microscope (Olympus Corporation; magnification, x400). Samples were incubated with anti-CD16 (1:200; cat. no. ab46629), anti-iNOS (1:200; cat. no. ab53769), anti-CD206 (1:200; cat. no. ab64693) and anti-Arg-1 primary antibodies (1:200; cat. no. ab133543) for 2 h at 37˚C. Biotinylated goat anti-rabbit/mouse IgG secondary antibodies (1:1,000; cat. no. KIT-9998; Fuzhou Maixin Biotech Co., Ltd) were added for 60 min at 37˚C.

Cell culture and chemicals. The human leukemia monocytic cell line (THP-1), the 293T cell line and the HepG2 and MHCC97H cell lines were purchased from The Cell Bank of Type Culture Collection of The Chinese Academy of Sciences. THP-1 cells were cultured in RPMI-1640 medium (Gibco; Thermo Fisher Scientific, Inc.) supplemented with 10% fetal calf serum (Gibco; Thermo Fisher Scientific, Inc.) and 0.05 mM β-mercaptoethanol (Sigma-Aldrich; Merck KGaA). 293T, HepG2 and MHCC97H cell lines were cultured in high-glucose DMEM (Gibco; Thermo Fisher Scientific, Inc.) supplemented with 10% fetal calf serum. All cell lines were cultured with 5% CO_2 at 37˚C.

Cell transfection. The third generation of lentiviral vector (hU6-MCS-Ubiquitin-EGFP-IRES-puromycin) containing short hairpin (sh)RNAs against TREM1 (shTREM1) used in the present study were produced by Shanghai GeneChem Co., Ltd., and were used for TREM1 gene knockdown. The target sequences of shRNAs were as follows: shTREM1-1, 5'-AGC CAGAAAGCTTGGCAGATA-3'; shTREM1-2, 5'-GAG GATCATACTAGAAGACTA-3'; and shTREM1-3, 5'-GTG GAAGATTCTGGACTGTAT-3'. Three plasmids (Shanghai GeneChem Co., Ltd.), namely 20 μg GV248 carrying the target sequence, 15 μg pHelper1.0 (carrying gag, pol and rev genes) and 10 μg pHelper2.0 (carrying the VSV-G gene), were mixed with Lipofectamine® 2000 (cat. no. 11668030; Invitrogen; Thermo Fisher Scientific, Inc.) for 15 min at room temperature. Subsequently, the mixture was transfected into 293T cells for 6 h at 37˚C to produce lentivirus. Lentiviral particles were collected and the virus titer were detected to be $2x10^9$ TU/ml. Transfections of shRNA into THP-1 cells were performed using polybrene (cat. no. REVG0001; Shanghai GeneChem Co., Ltd.) according to the manufacturer's instructions, and lentivirus at a multiplicity of infection of 50 was chosen for further experiments. After 12 h at 37˚C, the medium was changed into RPMI-1640 medium supplemented with 10% fetal calf serum and 0.05 mM β-mercaptoethanol containing no virus. The fluorescence intensity was observed under a fluorescence microscope at x100 and x400 magnification. Puromycin (5 μg/ml) was used to screen the shRNA-transfected THP-1 cells after 7 days at 37˚C. The knockdown efficiency of shTREM1 was tested by quantitative PCR assay and western blot analysis. A scrambled non-specific shRNA (5'-TTCTCCGAACGTGTCACGT-3') was used as a negative control (sh-ctrl).

Induced M2 macrophages from THP-1 cells. M2 macrophages were derived from THP-1 cells. shTREM1-treated macrophages were derived from shTREM1 THP-1 cells stimulated with 100 ng/ml phorbol 12-myristate 13-acetate (PMA; Sigma-Aldrich; Merck KGaA) for 24 h at 37˚C. After PMA treatment, 20 ng/ml IL-4 and 20 ng/ml IL-13 (PeproTech, Inc.) were added for 24 h at 37˚C (25).

Conditioned medium preparation. After incubating M2 and shTREM1 macrophages with fresh RPMI-1640 medium for an additional 24 h at 37˚C, the cells' conditioned media (CM) was harvested, centrifuged at 3,000 x g for 15 min at 37˚C, filter-sterilized through a 0.22-μm nylon filter (Nalgene; Thermo Fisher Scientific, Inc.) and finally stored at -80˚C for further experiments.

Double-labeling cells immunofluorescence. For immunofluorescence double labeling, cells were fixed in 4% paraformaldehyde for 20 min at 37˚C and permeabilized with 0.1% Triton X-100 for 10 min at 37˚C. After blocking non-specific binding with 0.1% BSA for 30 min at 37˚C, cells were incubated with primary antibodies against CD163 (cat. no. ab156769; Abcam) and TREM1 antibody (1:200; cat. no. YT5133; ImmunoWay Biotechnology Company) at a 1:500 dilution overnight at 4˚C. Subsequently, the samples were incubated with Alexa Fluor® 488-labeled donkey anti-rabbit IgG antibody (1:1,000; cat. no. A-21206; Thermo Fisher Scientific, Inc.) and Alexa Fluor® 546-labeled donkey anti-mouse IgG antibody (1:1,000; cat. no. A-10036; Thermo Fisher Scientific, Inc.) for 30 min at room temperature, and 1 μg/ml DAPI (Invitrogen; Thermo Fisher Scientific, Inc.) was used for nuclear labeling for 5 min at room temperature. Images of the labeled specimens were captured with a Zeiss confocal laser scanning microscope (Carl Zeiss AG) at x2,000 magnification and analyzed using ImageJ software. All treatments were performed in triplicate.

Reverse transcription-quantitative (RT-q)PCR. Total cellular RNA was extracted using TRIzol® reagent (Invitrogen; Thermo Fisher Scientific, Inc.) and was reverse transcribed into cDNA using PrimeScript™ 1st strand cDNA synthesis kit (cat. no. 6110A; Takara Bio, Inc.) according to the manufacturer's protocol. Subsequently, qPCR was performed using a SYBR Green kit (Takara Bio, Inc.) with specific primers for TREM1, iNOS, CD16, IL-12, CD163, Arg-1, IL-10 and GAPDH (used as the reference gene). PCR settings were adjusted according to the manufacturer's instructions: Initial denaturation at 95˚C for 30 sec and 40 cycles at 95˚C for 5 sec and 60˚C for 30 sec. All samples were assayed in triplicate and relative mRNA expression was quantified using the $2^{-\Delta\Delta Cq}$ method (26). The primer sequences used were as follows: TREM1 forward, 5'-GGCAGATAATAAGGGACGGAGAG-3' and reverse, 5'-CATTCGGACGCGCAGTAAA-3'; iNOS forward, 5'-GAG CCAGGCCACCTCTATGT-3' and reverse, 5'-GTCCTCGAC CTGCTCCTCAT-3'; CD16 forward, 5'-CCAGTGTGGCAT CATGTGG-3' and reverse, 5'-ATTGAGGCTCCAGGAACA CC-3'; IL-12 forward, 5'-CTGAAGAAGATGGTATCACCT GGAC-3' and reverse, 5'-TTAGAACCTCGCCTCCTTTGT G-3'; CD163 forward, 5'-TTCCTGTTCTGGACGTGTGG-3' and reverse, 5'-AGCTGGACCACAGCCAAGTT-3'; Arg-1 forward, 5'-GGTGTTGCCTGCTGCCTTCC-3' and reverse, 5'-GTTCTGAAGAGGTGAGTGGCTGTC-3'; IL-10 forward, 5'-TCAGAGAGGGGGTTAGACCTG-3' and reverse, 5'-GAG TTGGTCCTGCCAGACTT-3'; GAPDH forward, 5'-CCCTTC ATTGACCTCAACTACATG-3' and reverse, 5'-TGGGAT TTCCATTGATGACAAGC-3'.

Western blotting. Cells were washed with cold PBS, and then lysed with radioimmunoprecipitation assay buffer with phenylmethylsulfonyl fluoride (Beyotime Institute of Biotechnology). Cell lysates were collected and then centrifuged at 12,000 x g for 15 min at 4˚C. The bicinchoninic acid method was used to detect protein sample concentrations. A total of 20 μg protein/lane was separated via 10% SDS-PAGE, and the proteins were transferred to polyvinylidene fluoride membranes. The membranes were blocked against non-specific binding with 5% non-fat milk for 30 min at 37˚C, followed by overnight incubation at 4˚C with primary antibodies (all 1:1,000) against TREM1 (cat. no. YT5133; ImmunoWay Biotechnology Company), iNOS (cat. no. ab53769), CD16 (cat. no. ab46629), IL-12 (cat. no. ab106270), CD163 (cat. no. ab156769), Arg-1 (cat. no. ab133543), IL-10 (cat. no. ab34843), phosphorylated (p)-PI3K (cat. no. ab138364), p-AKT (ab183758), p-mTOR (cat. no. ab84400), PI3K (cat. no. ab151549), AKT (cat. no. ab179463), mTOR (cat. no. ab2732), snail (cat. no. ab229701), E-cadherin (cat. no. ab15148) and GAPDH (cat. no. ab181602) (all Abcam). After three washes with

TBS with 0.3% Triton X-100, the membranes were incubated with secondary HRP-conjugated goat anti-rabbit IgG (cat. no. ab6721) or goat anti-mouse IgG (cat. no. ab6789) secondary antibodies (both 1:2,000; Abcam) for 1 h at room temperature. The membranes were then washed three times and exposed via enhanced chemiluminescence reagents (BeyoECL Moon kit; cat. no. P0018FS; Beyotime Institute of Biotechnology). The protein bands were captured using Invitrogen iBright FL1500 Imaging System (Thermo Fisher Scientific, Inc.) and analyzed using ImageJ software.

Cell migration/invasion co-culture assay. Transwell chambers (8-μm; EMD Millipore) were used to evaluate cancer cell migration and invasion as previously described (27). A total of 80 μl high-glucose DMEM (Gibco; Thermo Fisher Scientific, Inc.) supplemented with 2% fetal calf serum (Gibco; Thermo Fisher Scientific, Inc.) containing $2x10^5$ HepG2 and MHCC97H cells was added into the upper chamber inserts. Serum-free RPMI-1640 medium, M2 macrophage-CM, shTREM1 macrophage-CM and sh-ctrl macrophage-CM were added into the bottom chambers to evaluate their influence on cancer cell migration. Before seeding HepG2 and MHCC97H cells, Matrigel (100 μl; Becton, Dickinson and Company) was placed into the upper chamber for invasion assays for 4 h at 37˚C, and the remaining steps were the same as for migration. After a 24-h incubation at 37˚C, the upper inserts were washed three times in PBS, fixed with 4% formaldehyde for 20 min at 37˚C and stained with crystal violet for 2 h at 37˚C. Five fields of view were randomly photographed with an Olympus CX41 light microscope (Olympus Corporation; magnification, x100) and the numbers of migrated and invaded cells per field were determined using ImageJ software.

Gap closure assay. A total of $2x10^5$ HepG2 and MHCC97H cells were seeded into culture inserts (Ibidi GmbH); the culture inserts were then removed, and a 500-μm wide gap was generated. Cells were incubated with serum-free RPMI-1640 medium, M2 macrophage-CM, shTREM1 macrophage-CM and sh-ctrl macrophage-CM for 24 h at 37˚C. Five fields of view were randomly photographed with an Olympus CX41 light microscope (Olympus Corporation; magnification, x100) and the gap closure rate was estimated by calculating the gap area with ImageJ software.

Cell proliferation assay. HepG2 and MHCC97H cells were seeded into 96-well plates at a density of $1x10^4$ cells/well. Cells were incubated with serum-free RPMI-1640 medium, M2 macrophage-CM, shTREM1 macrophage-CM and sh-ctrl macrophage-CM for 24 h at 37˚C. According to the instructions of a BrdU Cell Proliferation Assay kit (cat. no. 6813; Cell Signaling Technology, Inc.), BrdU was added to wells and incubated for 12 h at 37˚C. Subsequently, cells were fixed and denatured using 100 μl Fix/Denature solution (part of the aforementioned kit) for 30 min at 37˚C. Cells were washed with cold PBS three times. Cells were incubated with 100 μl anti-BrdU antibody (part of the aforementioned kit) for 1 h at 37˚C and were then washed three times with cold PBS. Subsequently, HRP-conjugated secondary antibody (part of the aforementioned kit) was added for 1 h at 37˚C. A total of 100 μl Substrate Solution was then added and incubated for 5 min at 37˚C. Finally, 100 μl Stop Solution was added to stop the enzyme reaction, and the levels of BrdU incorporation was determined using an ELISA reader at a wavelength of 450 nm (Bio-Rad Laboratories, Inc.).

Statistical analysis. All continuous variables were presented as the mean ± SD. The paired Student's t-test was used for comparative analysis of paired cancerous and adjacent normal tissues. The unpaired Student's t-test was applied for comparisons between 2 groups for the other assays, and one-way ANOVA followed by Tukey's multiple comparison test was used when >2 groups were evaluated. Two-sided $P<0.05$ was considered to indicate a statistically significant difference. All statistical analysis was performed using SPSS version 19.0 (IBM Corp.).

Results

High TREM1 expression on M2 macrophages in HCC. The clinical characteristics of the study population are described in Table SI. Immunohistochemistry was performed to determine the expression levels of TREM1 in HCC tissues and adjacent normal tissues. The percentage of $TREM1^+$ cells per field in HCC tissues was significantly higher than that in adjacent normal tissues (11.23±0.8840 vs. 2.253±0.8662%; $P<0.01$; Fig. 1A-C). Immunohistochemical double staining was used to detect the tumor-associated macrophage phenotype in HCC by analyzing CD206 and Arg-1 expression. The results revealed that the infiltration of M2 macrophages in liver cancer tissues was significantly increased compared with that in adjacent normal tissues (3.50±0.5000 vs. 0.5100±0.1813%; $P<0.01$; Fig. 1D-F). No double-positive cells of CD16 and iNOS (M1-associated markers) were observed, indicating no M1 macrophage infiltration in liver cancer tissues and adjacent normal tissues (Fig. 1G-I). In addition, immunohistochemical double staining with the M2 macrophage surface markers CD206 and TREM1 revealed that TREM1 was highly expressed on the surface of M2 macrophages in HCC tissues (16.51±0.9327 vs. 6.644±1.221%; $P<0.01$; Fig. 1J-L). The current results suggested that M2 macrophages mainly infiltrate HCC tissues, while no infiltration of M1 macrophages was observed in both HCC and adjacent normal tissues. M2 macrophages in HCC tissues highly express TREM1. These results indicated that TREM1 expression on M2 macrophages may serve an important role in the progression of HCC.

M2 macrophages induced from human leukemia monocytic cells. To establish a model of human M2 macrophages, human leukemia monocytic cells (THP-1) were stimulated using PMA, IL-4 and IL-13. Double-immunofluorescence labeling was used to identify co-expression of CD163 and TREM1 in M2 macrophages (Fig. 2A). RT-qPCR and western blot analysis revealed that TREM1 expression in M2 macrophages was significantly higher than in THP-1 cells (Fig. 2B and C). The mRNA expression levels of iNOS, CD16 and IL-12 (M1 macrophage-associated markers) were not significantly different between THP-1 cells and M2 macrophages, while the expression levels of CD163, Arg-1 and IL-10 (M2 macrophage-associated markers) were significantly increased in M2 macrophages compared with in THP-1 cells (Fig. 2D and E). Similarly, protein expression levels of iNOS, CD16 and IL-12 exhibited no significant difference between THP-1 cells and M2 macrophages, while protein expression

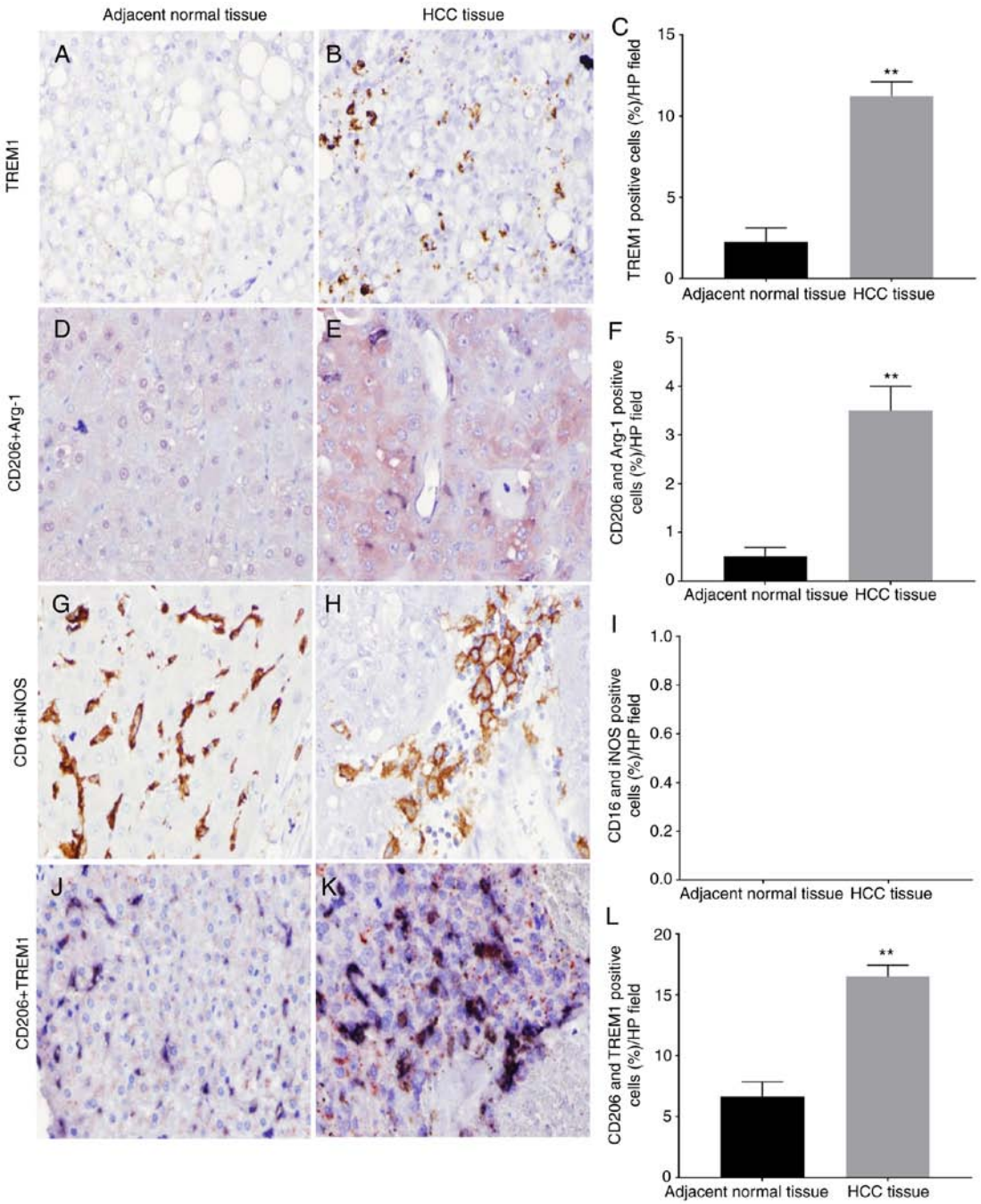

Figure 1. TREM1/macrophage-associated marker expression in HCC and adjacent normal tissues. Images were captured at x400 magnification. TREM1 expression in (A) normal and (B) HCC tissues. Some pale-stained brown precipitate was observed outside the cell membrane in adjacent tissues, but a large number of brown-black precipitates were observed on the cell membrane in HCC tissues. (C) Quantification of TREM1 expression. M2 macrophage-associated markers (CD206 and Arg-1) in (D) normal and (E) HCC tissues. The blue-black precipitate on the membrane was positive for CD206, and the red precipitate in the cytoplasm was positive for Arg-1. Cells labeled with two colors (both markers) were M2 macrophages. (F) Quantification of $CD206^+$ and $Arg\text{-}1^+$ cells. M1 macrophage-associated markers (CD16 and iNOS) in (G) normal and (H) HCC tissues. The brown and black precipitates on the cell membrane were positive for CD16, no red precipitates for iNOS were found in the cytoplasm and nuclei, indicating that there were no double-positive cells for CD16 and iNOS. (I) Quantification of $CD16^+$ and $iNOS^+$ cells. TREM1 expression on the surface of M2 macrophages in (J) normal and (K) HCC tissues. The blue-black precipitate on the membrane was positive for CD206, and the red precipitate was positive for TREM1. (L) Quantification of $CD206^+$ and $TREM1^+$ cells. $^{**}P<0.01$. HCC, hepatocellular carcinoma; TREM1, triggering receptor expressed on myeloid cells-1; iNOS, inducible nitric oxide synthase; Arg-1, arginase-1; HP, high power.

levels of CD163, Arg-1 and IL-10 were significantly upregulated in M2 macrophages compared with in THP-1 cells (Fig. 2F). Overall, the present data indicated that M2 macrophages were successfully induced from the THP-1 monocytic cell line.

Downregulation of TREM1 inhibits M2 macrophage polarization and promotes a shift towards the M1 phenotype. To discover possible functions of TREM1 in macrophage polarization, shRNAs were used to knock down TREM1 expression. As shown in Fig. 3A, shTREM1-2 was the most effective at TREM1 silencing and stable regulation of TREM1 in THP-1 cells and was therefore used for subsequent experiments. Western blot analysis revealed that transfection with shTREM1-2 resulted in a significant downregulation of

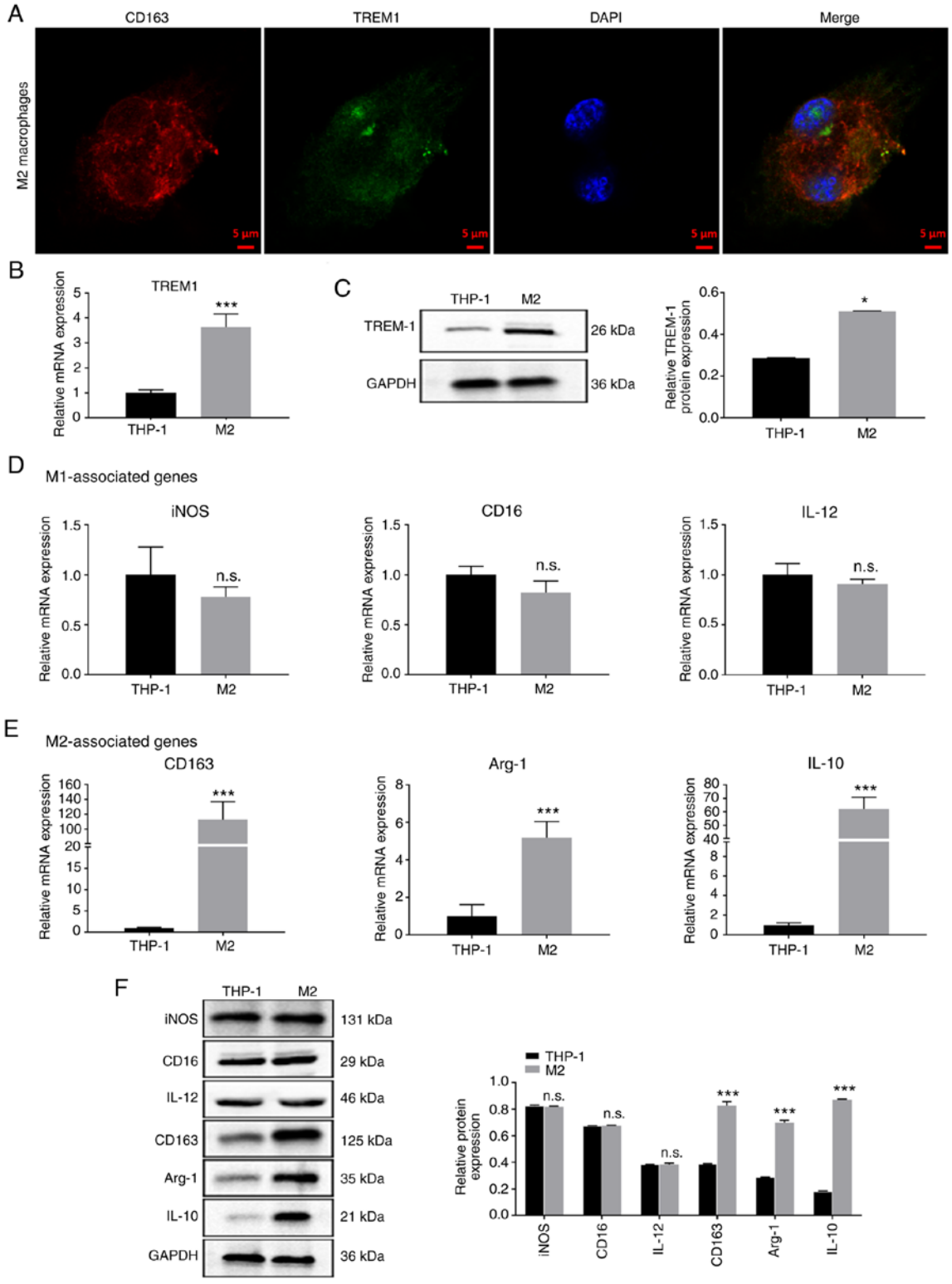

Figure 2. M2 macrophages induced from human leukemia monocytic THP-1 cells. M2 macrophages derived from THP-1 cells were stimulated using phorbol 12-myristate 13-acetate, IL-4 and IL-13 for 24 h. (A) Representative immunofluorescence images showing co-localization of CD163 (red) and TREM1 (green) in M2 macrophages (scale bar, 5 μm). TREM1 expression was assessed by (B) RT-qPCR and (C) western blotting. (D) mRNA expression levels of the M1 macrophage markers iNOS, CD16 and IL-12 were measured by RT-qPCR. (E) mRNA expression levels of the M2 macrophage markers CD163, Arg-1 and IL-10 were examined via RT-qPCR. (F) Protein expression levels of M1 and M2 macrophage markers were determined by western blotting. Data are shown as the mean ± SD of three independent experiments. *P<0.05 and ***P<0.001 vs. THP-1. n.s., no significance; iNOS, inducible nitric oxide synthase; Arg-1, arginase-1; TREM1, triggering receptor expressed on myeloid cells-1; RT-qPCR, reverse transcription-quantitative PCR.

TREM1 expression compared with sh-ctrl-transfected cells (Fig. 3B). RT-qPCR and western blot analysis demonstrated that iNOS, CD16 and IL-12 expression was significantly upregulated in shTREM1 macrophages, while CD163, Arg-1 and IL-10 expression was significantly downregulated in shTREM1 macrophages compared with in sh-ctrl macrophages

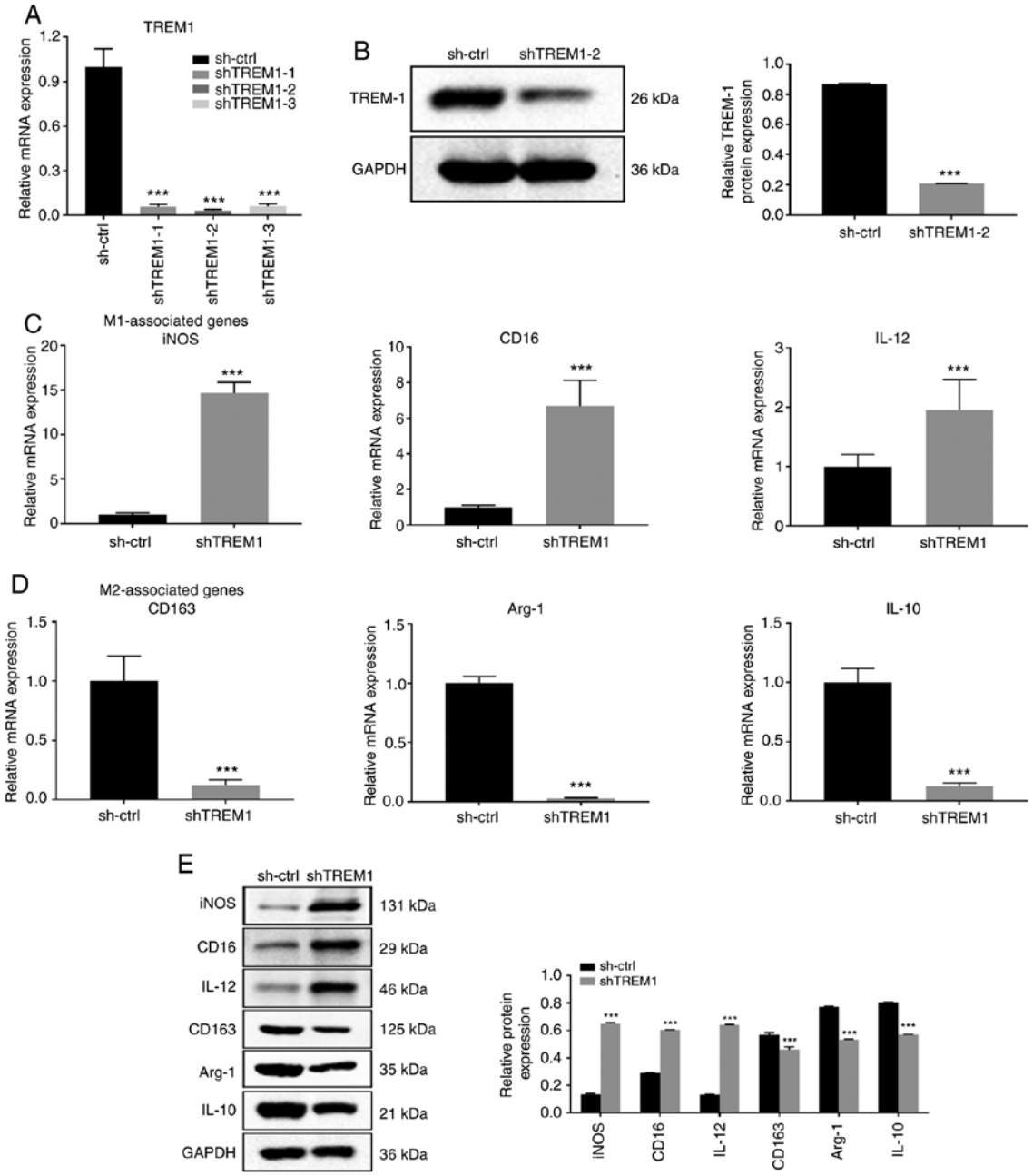

Figure 3. Downregulation of TREM1 in macrophages inhibits M2 polarization and shifts macrophages into an M1 phenotype. shRNA against TREM1 was used in THP-1 cells. M2 macrophages were derived from THP-1 cells, and shTREM1 macrophages were derived from shTREM1 THP-1 cells with stimulation using phorbol 12-myristate 13-acetate, IL-4 and IL-13 for 24 h. (A) shTREM1-1, shTREM1-2 and shTREM1-3 were used for TREM1-knockdown. TREM1 mRNA expression was assessed via RT-qPCR. (B) TREM1 protein expression was assessed by western blotting. (C) mRNA expression levels of the M1 macrophage-associated markers (iNOS, CD16 and IL-12) and (D) M2 macrophage-associated markers (CD163, Arg-1 and IL-10) were measured by RT-qPCR. (E) Protein expression levels of M1 and M2 macrophage-associated markers were determined by western blotting. Data are shown as the mean ± SD of three independent experiments. ***P<0.001 vs. sh-ctrl. shRNA, short hairpin RNA; ctrl, control; iNOS, inducible nitric oxide synthase; Arg-1, arginase-1; TREM1, triggering receptor expressed on myeloid cells-1; RT-qPCR, reverse transcription-quantitative PCR.

(Fig. 3C-E). Overall, the present results indicated that TREM1 downregulation inhibited M2 macrophage polarization and promoted a shift towards the M1 phenotype.

Downregulation of TREM1 in macrophages inhibits the migration and invasion of tumor cells. A co-culture system was used to investigate the effect of shTREM1 macrophages on the migration and invasion of cancer cells. The results revealed that M2 macrophage-CM (M2-CM) significantly increased cell gap closure (Fig. 4A), as well as migration and invasion (Fig. 4B), in HepG2 and MHCC97H cell lines compared with RPMI-1640 medium (1640); meanwhile, shTREM1 macrophage-CM (shTREM1-CM) significantly decreased this effect. The present results indicated that downregulation of TREM1 can inhibit the migration and invasion of tumor cells.

Downregulation of TREM1 in macrophages inhibits epithelial-mesenchymal transition (EMT) and the proliferation of tumor cells. A co-culture system was used to investigate the effect of shTREM1 macrophages on EMT of cancer cells.

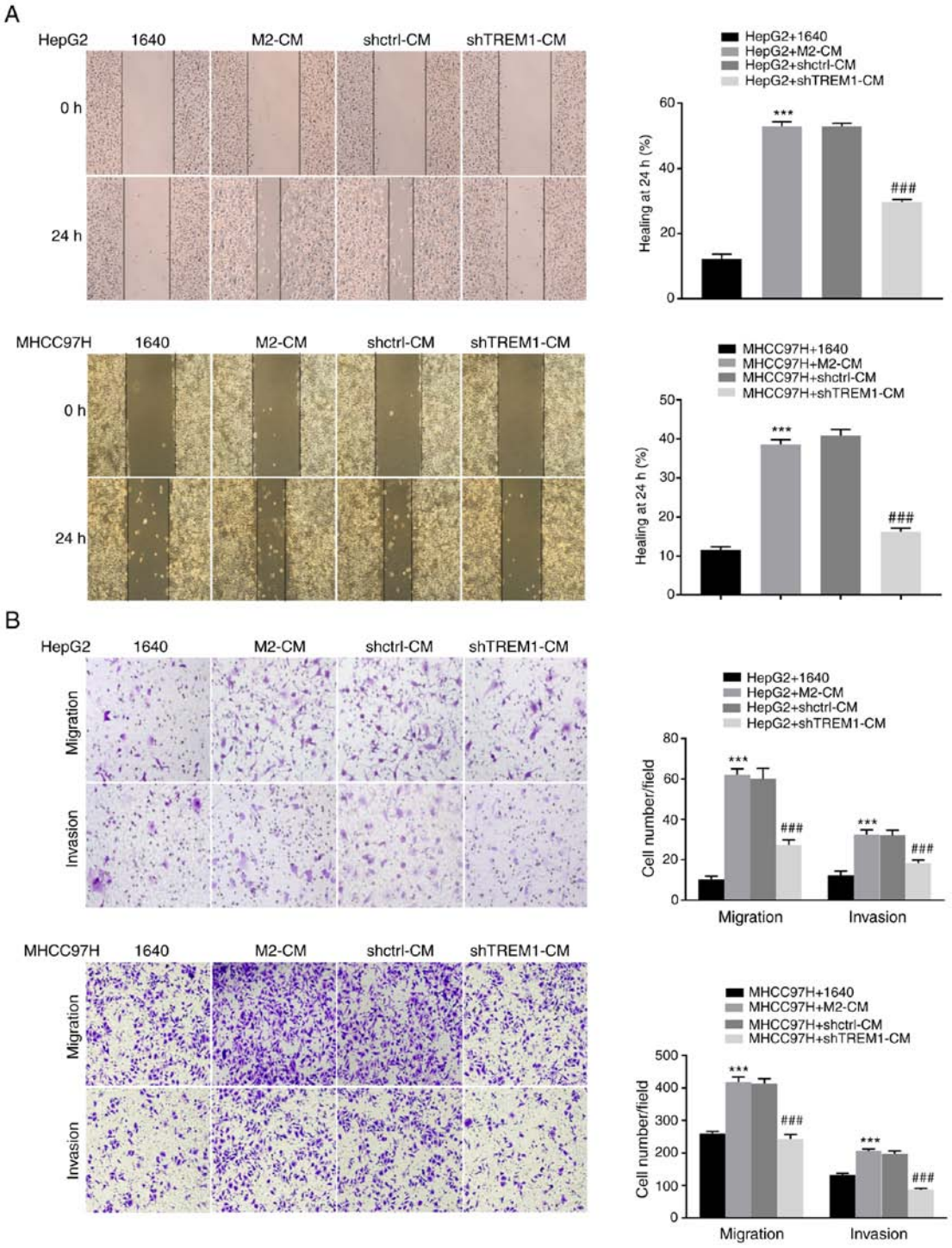

Figure 4. Downregulation of TREM1 in macrophages inhibits the migration and invasion of liver cancer cells. HepG2 and MHCC97H cell lines were co-cultured with RPMI-1640 medium (1640), M2 macrophages-CM (M2-CM), shTREM1 macrophages-CM (shTREM1-CM) and sh-ctrl macrophages-CM (shctrl-CM). Effects of downregulation of TREM1 in macrophages during the migration and invasion of HepG2 and MHCC97H cells were detected using (A) gap closure and (B) Transwell migration and invasion assays (magnification, x100). Data are shown as the mean ± SD of three independent experiments. ***P<0.001 vs. 1640. $^{###}$P<0.001 vs. shctrl-CM. sh, short hairpin; ctrl, control; TREM1, triggering receptor expressed on myeloid cells-1; CM, conditioned medium.

The results revealed that M2-CM significantly increased the protein expression levels of snail and significantly decreased those of E-cadherin in HepG2 (Fig. 5A) and MHCC97H (Fig. 5B) cells compared with RPMI-1640 medium; meanwhile, shTREM1-CM reversed this effect. These results indicated that downregulation of TREM1 inhibited the EMT of tumor cells. A BrdU kit was used to investigate the effect of shTREM1 macrophages on the proliferation of cancer cells. The results demonstrated that M2-CM significantly increased proliferation of HepG2 and MHCC97H cells compared with RPMI-1640 medium; meanwhile, shTREM1-CM reversed this effect (Fig. 5C). The present results indicated that downregulation of TREM1 inhibited the proliferation of tumor cells.

Downregulation of TREM1 inhibits PI3K/AKT signaling in the M2 polarization of macrophages. To discover the molecular

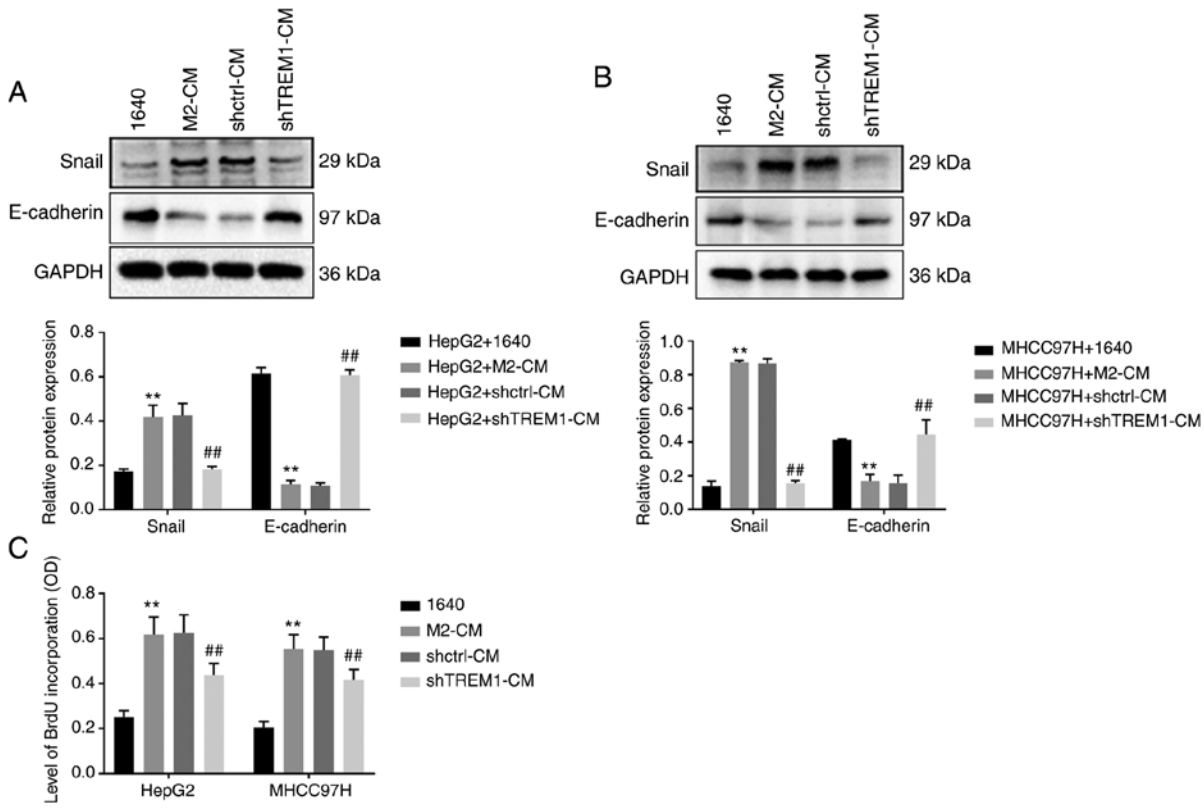

Figure 5. Downregulation of TREM1 in macrophages inhibits EMT and proliferation of liver cancer cells. HepG2 and MHCC97H cell lines were co-cultured with RPMI-1640 medium (1640), M2 macrophages-CM (M2-CM), shTREM1 macrophages-CM (shTREM1-CM) and sh-ctrl macrophages-CM (shctrl-CM). Protein expression levels of snail and E-cadherin in (A) HepG2 and (B) MHCC97H cells were examined by western blot analysis. (C) Effects of downregulation of TREM1 in macrophages during the proliferation of HepG2 and MHCC97H cells were detected using a BrdU kit. Data are shown as the mean ± SD of three independent experiments. **P<0.01 vs. 1640. $^{\#\#}$P<0.01 vs. shctrl-CM. sh, short hairpin; ctrl, control; TREM1, triggering receptor expressed on myeloid cells-1; CM, conditioned medium; OD, optical density.

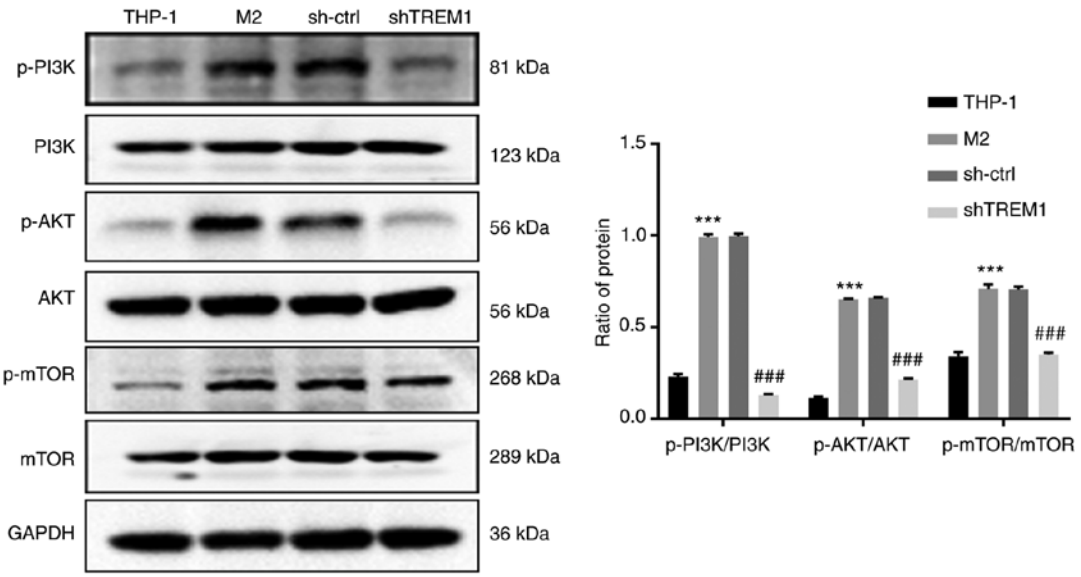

Figure 6. Downregulation of TREM1 in macrophages inhibits PI3K/AKT signaling in the M2 polarization of macrophages. M2 macrophages were derived from THP-1 cells, and shTREM1 macrophages were derived from shTREM1 THP-1 cells. Protein expression levels of p-PI3K(p85), PI3K, p-AKT, AKT, p-mTOR and mTOR were examined by western blot analysis. Data are shown as the mean ± SD of three independent experiments. ***P<0.001 vs. THP-1. $^{\#\#\#}$P<0.001 vs. sh-ctrl. sh, short hairpin; ctrl, control; TREM1, triggering receptor expressed on myeloid cells-1; p, phosphorylated.

mechanisms of the effects of silencing TREM1 in macrophages and inhibition of M2 polarization of macrophages, western blotting was used to determine the protein expression levels of p-PI3K (p85), PI3K, p-AKT, AKT, p-mTOR and mTOR. As illustrated in Fig. 6, the ratios of p-PI3K/PI3K, p-AKT/AKT and p-mTOR/mTOR were significantly upregulated in M2-polarized

macrophages, while downregulation of TREM1 in macrophages reversed this effect. These results indicated that the PI3K/AKT/mTOR signaling pathway may be involved in the regulation of macrophage polarization by TREM1.

Discussion

The TME is a complex and dynamic cellular system that is associated with cancer occurrence, progression and response to therapy (28). TAMs are predominant inflammatory components in the TME and can exist as classically activated macrophages (M1 macrophages) and alternatively activated macrophages (M2 macrophages) in response to different stimuli within the TME (10). In numerous types of cancer, such as ovarian, breast and pancreatic cancer, TAMs tend to exhibit M2 polarization characteristics (10,13). The functions of M2 macrophages in cancer are complex, including promotion of angiogenesis, enhancing cell proliferation, migration and invasion, and suppression of the immune response in the TME (29). Yeung *et al* (14) revealed that M2 macrophages promote tumor growth and invasiveness in HCC through CCL2-induced EMT.

HCC is a well-known and extensively investigated inflammation-associated cancer (8,9). TREM1 is regarded as an effective amplifier of inflammatory responses in the immunoglobulin superfamily (30). Previous studies have investigated TREM1 expression in HCC cells and hepatic stellate cells (31,32). Duan and Wang (31) reported that the influence of TREM1 expression on HCC cell proliferation, invasion and apoptosis was not mediated by monocytes or macrophages, indicating that TREM1 had a direct pro-tumor effect in cancer cells. The present study confirmed that TREM1 expression was elevated in tumor tissues of patients with HCC. Furthermore, the current results revealed that TREM1 was highly expressed in M2 macrophages in HCC tissues through immunohistochemical double-staining with the surface markers CD206 and TREM1. This result indicated that TREM1 may have an indirect effect on HCC mediated by macrophages. The activation of TREM1 expression in Kupffer cells (resident macrophages in liver tissue) stimulates tumorigenesis during diethylnitrosamine-induced hepatocarcinogenesis (22). Therefore, TREM1 expression on macrophages may serve an important role in HCC formation.

Recruited monocyte-derived macrophages are thought to be more plastic and prone to switch from an antitumor to a pro-tumor phenotype under the influence of the growing tumor cells (33). These phenotypes are usually defined by the M1/M2 polarization classification and different functional patterns. As a pro-inflammatory receptor, TREM1 protein expression on macrophages may serve as a regulator to switch the phenotype of macrophages and change their function (34). The cross-talk between TREM1 and macrophages in the TME during liver cancer development remains poorly understand. To explore the mechanisms by which TREM1 influences macrophage polarization, the present study knocked down TREM1 expression in macrophages by shRNA, revealing that M2 polarization markers were inhibited and M1 macrophage-associated markers were upregulated in shTREM1 macrophages. The present results suggested that downregulation of TREM1 may promote a shift in shTREM1 macrophages towards the M1 phenotype, presenting as iNOS upregulation and Arg-1 downregulation. Additionally, the CM from TREM1-knockdown macrophages was co-cultured with liver cancer cells, as well as the CM from M2 macrophages used as a control group. Blocking TREM1 shifted the polarization of macrophages to inhibit migration, invasion, EMT and proliferation of liver cancer cells. Similarly, a recent study has found that lncRNA cox-2 small interfering RNA decreases the ability of M1 macrophages to inhibit tumor cell proliferation, invasion, migration and EMT, while strengthening the ability of M2 macrophages to promote tumor cell proliferation and inhibit apoptosis (35). Therefore, the present results provided evidence for macrophage polarization in the TME, which increases the current understanding of the role of TAMs in cancer progression. The current study further defined phenotypic transition as one of the major mechanisms by which TREM1 signaling may act on activated M2 macrophages to drive hepatocarcinogenesis. Notably, TAMs are being identified as increasingly complex, with several studies suggesting that distinct populations may have different roles in tumorigenesis (22,31).

The PI3K signaling pathway is a classical signaling pathway that converges inflammatory and metabolic signals during phagocytosis, autophagy and cell metabolism (36,37). Class IA PI3K includes a p110 catalytic subunit, which interacts with an SH2 domain-containing p85 regulatory subunit (36,37). The p85 regulatory subunit representative of PI3K phosphorylation was assessed in the present study. Phosphorylation of PI3K results in the activation of downstream signal effectors, including AKT and mTOR; PI3K/AKT and its downstream effectors are regarded as central mediators of the inflammatory response and polarization of macrophages (38). In bone marrow-derived macrophages, the PI3K/AKT signaling pathway promotes M2 polarization (39), while inhibition of either PI3K or AKT attenuates the expression levels of M2-associated genes (39,40), illustrating the importance of the PI3K/AKT signaling pathway in M2 polarization. The present findings suggested that TREM1 regulated macrophage polarization through the PI3K/AKT signaling pathway. Upregulated expression levels of markers of PI3K/AKT signaling pathway activation were detected in the current study, suggesting that the M2 macrophage polarization depended on this activation. In addition, downregulation of TREM1 in macrophages blocked the activation of PI3K/AKT signaling in M2 polarization. Although the present results do not formally prove a cause-effect association, they clearly support that the PI3K/AKT signaling pathway may partially mediate an M1/M2 phenotypic switch in the TME. A limitation of the present study is that it was only demonstrated that TREM1 inhibited liver cancer cells by regulating macrophage polarization. The function of TREM-1$^+$ TAMs and their relevant mechanisms of immunosuppression in the tumor microenvironment require further investigation.

In conclusion, the present study provided novel evidence that knocking down TREM1 expression may shift M2 macrophages towards a M1 phenotype, likely through PI3K/AKT signaling. These findings enhance the understanding of TREM1 expression on M2 macrophages and its role in the pathogenesis of liver cancer. Finally, the present study supports targeting TREM1 and/or TAMs as a therapeutic strategy against cancer to improve the efficacy of current systemic therapy.

Acknowledgements

Not applicable.

Funding

The present study was supported by grants from the Middle-Aged Backbone Training Project in the Health System of Fujian province (grant no. 2016-ZQN-40) and the Startup Fund for scientific research of Fujian Medical University (grant no. 2017XQ1077).

Availability of data and materials

The datasets generated and/or analyzed during the current study are not publicly available due to restrictions of the First Affiliated Hospital of Fujian Medical University, but are available from the corresponding author on reasonable request.

Authors' contributions

MC completed most of the experiments and wrote the manuscript. QZ designed the study and reviewed/edited the drafts. RL analyzed the data, completed part of the experiments and edited the drafts. XL and WC performed follow-up of patients and collected data. HW completed the immunohistochemical analysis and co-wrote the final draft. MC, RL and QZ were responsible for the authenticity of the data. QZ is the guarantor of this work and, as such, had full access to all the data in the study and takes responsibility for the integrity of the data and the accuracy of the data analysis. All authors read and approved the final manuscript.

Ethics approval and consent to participate

All patients signed informed consent forms in accordance with the Declaration of Helsinki. The study protocol was approved by the Ethical Committee of The First Affiliated Hospital of Fujian Medical University [Fuzhou, China; approval no. (2015) 132].

Patient consent for publication

Not applicable.

Competing interests

The authors declare that they have no competing interests.

References

1. Dawkins J and Webster RM: The hepatocellular carcinoma market. Nat Rev Drug Discov 18: 13-14, 2019.
2. Ryerson AB, Eheman CR, Altekruse SF, Ward JW, Jemal A, Sherman RL, Henley SJ, Holtzman D, Lake A, Noone AM, *et al*: Annual report to the nation on the status of cancer, 1975-2012, featuring the increasing incidence of liver cancer. Cancer 122: 1312-1337, 2016.
3. Ferlay J, Soerjomataram I, Dikshit R, Eser S, Mathers C, Rebelo M, Parkin DM, Forman D and Bray F: Cancer incidence and mortality worldwide: Sources, methods and major patterns in GLOBOCAN 2012. Int J Cancer 136: E359-E386, 2015.
4. Bray F, Ferlay J, Soerjomataram I, Siegel RL, Torre LA and Jemal A: Global cancer statistics 2018: GLOBOCAN estimates of incidence and mortality worldwide for 36 cancers in 185 countries. CA Cancer J Clin 68: 394-424, 2018.
5. Forner A, Reig M and Bruix J: Hepatocellular carcinoma. Lancet 391: 1301-1314, 2018.
6. Bruix J, Qin S, Merle P, Granito A, Huang YH, Bodoky G, Pracht M, Yokosuka O, Rosmorduc O, Breder V, *et al*: Regorafenib for patients with hepatocellular carcinoma who progressed on sorafenib treatment (RESORCE): A randomised, double-blind, placebo-controlled, phase 3 trial. Lancet 389: 56-66, 2017.
7. El-Khoueiry AB, Sangro B, Yau T, Crocenzi TS, Kudo M, Hsu C, Kim TY, Choo SP, Trojan J, Welling TH Rd, *et al*: Nivolumab in patients with advanced hepatocellular carcinoma (CheckMate 040): An open-label, non-comparative, phase 1/2 dose escalation and expansion trial. Lancet 389: 2492-2502, 2017.
8. Nikolaou K, Sarris M and Talianidis I: Molecular pathways: The complex roles of inflammation pathways in the development and treatment of liver cancer. Clin Cancer Res 19: 2810-2816, 2013.
9. Arzumanyan A, Reis HM and Feitelson MA: Pathogenic mechanisms in HBV- and HCV-associated hepatocellular carcinoma. Nat Rev Cancer 13: 123-135, 2013.
10. Solinas G, Germano G, Mantovani A and Allavena P: Tumor-associated macrophages (TAM) as major players of the cancer-related inflammation. J Leukoc Biol 86: 1065-1073, 2009.
11. Boniakowski AE, Kimball AS, Jacobs BN, Kunkel SL and Gallagher KA: Macrophage-mediated inflammation in normal and diabetic wound healing. J Immunol 199: 17-24, 2017.
12. Glass CK and Natoli G: Molecular control of activation and priming in macrophages. Nat Immunol 17: 26-33, 2016.
13. Binnemars-Postma K, Storm G and Prakash J: Nanomedicine strategies to target tumor-associated macrophages. Int J Mol Sci 18: 979, 2017.
14. Yeung OW, Lo CM, Ling CC, Qi X, Geng W, Li CX, Ng KT, Forbes SJ, Guan XY, Poon RT, *et al*: Alternatively activated (M2) macrophages promote tumour growth and invasiveness in hepatocellular carcinoma. J Hepatol 62: 607-616, 2015.
15. Capece D, Fischietti M, Verzella D, Gaggiano A, Cicciarelli G, Tessitore A, Zazzeroni F and Alesse E: The inflammatory microenvironment in hepatocellular carcinoma: A pivotal role for tumor-associated macrophages. Biomed Res Int 2013: 187204, 2013.
16. Sharif O and Knapp S: From expression to signaling: Roles of TREM-1 and TREM-2 in innate immunity and bacterial infection. Immunobiology 213: 701-713, 2008.
17. Tessarz AS and Cerwenka A: The TREM-1/DAP12 pathway. Immunol Lett 116: 111-116, 2008.
18. Read CB, Kuijper JL, Hjorth SA, Heipel MD, Tang X, Fleetwood AJ, Dantzler JL, Grell SN, Kastrup J, Wang C, *et al*: Cutting edge: Identification of neutrophil PGLYRP1 as a ligand for TREM-1. J Immunol 194: 1417-1421, 2015.
19. van Bremen T, Dromann D, Luitjens K, Dodt C, Dalhoff K, Goldmann T and Schaaf B: Triggering receptor expressed on myeloid cells-1 (Trem-1) on blood neutrophils is associated with cytokine inducibility in human *E. coli* sepsis. Diagn Pathol 8: 24, 2013.
20. Ho CC, Liao WY, Wang CY, Lu YH, Huang HY, Chen HY, Chan WK, Chen HW and Yang PC: TREM-1 expression in tumor-associated macrophages and clinical outcome in lung cancer. Am J Respir Crit Care Med 177: 763-770, 2008.
21. Shen ZT and Sigalov AB: Novel TREM-1 inhibitors attenuate tumor growth and prolong survival in experimental pancreatic cancer. Mol Pharm 14: 4572-4582, 2017.
22. Wu J, Li J, Salcedo R, Mivechi NF, Trinchieri G and Horuzsko A: The proinflammatory myeloid cell receptor TREM-1 controls Kupffer cell activation and development of hepatocellular carcinoma. Cancer Res 72: 3977-3986, 2012.
23. Tandon P, Abraldes JG, Keough A, Bastiampillai R, Jayakumar S, Carbonneau M, Wong E, Kao D, Bain VG and Ma M: Risk of bacterial infection in patients with cirrhosis and acute variceal hemorrhage, based on Child-Pugh class, and effects of antibiotics. Clin Gastroenterol Hepatol 13: 1189-1196.e2, 2015.
24. Llovet JM, Brú C and Bruix J: Prognosis of hepatocellular carcinoma: The BCLC staging classification. Semin Liver Dis 19: 329-338, 1999.
25. Genin M, Clement F, Fattaccioli A, Raes M and Michiels C: M1 and M2 macrophages derived from THP-1 cells differentially modulate the response of cancer cells to etoposide. BMC Cancer 15: 577, 2015.

26. Livak KJ and Schmittgen TD: Analysis of relative gene expression data using real-time quantitative PCR and the 2(-Delta Delta C(T). Methods 25: 402-408, 2001.
27. Zhang L, Wang JN, Tang JM, Kong X, Yang JY, Zheng F, Guo LY, Huang YZ, Zhang L, Tian L, *et al*: VEGF is essential for the growth and migration of human hepatocellular carcinoma cells. Mol Biol Rep 39: 5085-5093, 2012.
28. Polyak K, Haviv I and Campbell IG: Co-evolution of tumor cells and their microenvironment. Trends Genet 25: 30-38, 2009.
29. Condeelis J and Pollard JW: Macrophages: Obligate partners for tumor cell migration, invasion, and metastasis. Cell 124: 263-266, 2006.
30. Bouchon A, Dietrich J and Colonna M: Cutting edge: Inflammatory responses can be triggered by TREM-1, a novel receptor expressed on neutrophils and monocytes. J Immunol 164: 4991-4995, 2000.
31. Duan M, Wang ZC, Wang XY, Shi JY, Yang LX, Ding ZB, Gao Q, Zhou J and Fan J: TREM-1, an inflammatory modulator, is expressed in hepatocellular carcinoma cells and significantly promotes tumor progression. Ann Surg Oncol 22: 3121-3129, 2015.
32. Liao R, Sun TW, Yi Y, Wu H, Li YW, Wang JX, Zhou J, Shi YH, Cheng YF, Qiu SJ and Fan J: Expression of TREM-1 in hepatic stellate cells and prognostic value in hepatitis B-related hepatocellular carcinoma. Cancer Sci 103: 984-992, 2012.
33. Colegio OR, Chu NQ, Szabo AL, Chu T, Rhebergen AM, Jairam V, Cyrus N, Brokowski CE, Eisenbarth SC, Phillips GM, *et al*: Functional polarization of tumour-associated macrophages by tumour-derived lactic acid. Nature 513: 559-563, 2014.
34. Lo TH, Tseng KY, Tsao WS, Yang CY, Hsieh SL, Chiu AW, Takai T, Mak TW, Tarng DC and Chen NJ: TREM-1 regulates macrophage polarization in ureteral obstruction. Kidney Int 86: 1174-1186, 2014.
35. Ye Y, Xu Y, Lai Y, He W, Li Y, Wang R, Luo X, Chen R and Chen T: Long non-coding RNA cox-2 prevents immune evasion and metastasis of hepatocellular carcinoma by altering M1/M2 macrophage polarization. J Cell Biochem 119: 2951-2963, 2018.
36. Guillermet-Guibert J, Bjorklof K, Salpekar A, Gonella C, Ramadani F, Bilancio A, Meek S, Smith AJ, Okkenhaug K and Vanhaesebroeck B: The p110beta isoform of phosphoinositide 3-kinase signals downstream of G protein-coupled receptors and is functionally redundant with p110gamma. Proc Natl Acad Sci USA 105: 8292-8297, 2008.
37. Vergadi E, Ieronymaki E, Lyroni K, Vaporidi K and Tsatsanis C: Akt signaling pathway in macrophage activation and M1/M2 polarization. J Immunol 198: 1006-1014, 2017.
38. Byles V, Covarrubias AJ, Ben-Sahra I, Lamming DW, Sabatini DM, Manning BD and Horng T: The TSC-mTOR pathway regulates macrophage polarization. Nat Commun 4: 2834, 2013.
39. Rauh MJ, Ho V, Pereira C, Sham A, Sly LM, Lam V, Huxham L, Minchinton AI, Mui A and Krystal G: SHIP represses the generation of alternatively activated macrophages. Immunity 23: 361-374, 2005.
40. Ruckerl D, Jenkins SJ, Laqtom NN, Gallagher IJ, Sutherland TE, Duncan S, Buck AH and Allen JE: Induction of IL-4Rα-dependent microRNAs identifies PI3K/Akt signaling as essential for IL-4-driven murine macrophage proliferation in vivo. Blood 120: 2307-2316, 2012.